LaserCube Optical Communication Terminal for Nano and Micro Satellites*

Francesco Sansone[a,*], Alessandro Francesconi[a], Roberto Corvaja[b], Giuseppe Vallone[b], Riccardo Antonello[b], Francesco Branz[b], Paolo Villoresi[b]

[a] *Stellar Project Srl, via Niccolò Tommaseo 69, 35131 Padova, Italy*
[b] *Department of Information Engineering, University of Padova, via G. Gradenigo 6/B, 35131 Padova, Italy*

Abstract

This paper presents the design and testing of LaserCube, a miniature optical communication terminal conceived for nano and microsatellites. The system architecture has been defined for both the downlink and intersatellite link version of the system. Then, a complete engineering model of LaserCube in its intersatellite link configuration has been developed and tested. It features (1) a dual stage pointing and tracking system based on a coarse pointing mechanism patented by Stellar Project, (2) an optical head with a full–duplex telecom channel with transmission and reception on the same wavelength for two–way links, (3) a transceiver section with telecom laser source and optical receiver and (4) the terminal control unit with onboard computer, actuator drivers and data interface. Experimental validation of the system is achieved through a laboratory simulation of an intersatellite link scenario with realistic dynamic disturbance coming from the host satellite attitude jitter.

Keywords: Optical Communications, Intersatellite Link, Nanosatellite, CubeSat

1. Introduction

Over the last decade, the exploitation of small satellites, and especially CubeSats, for commercial applications has been constantly increasing, with new projects based on fleets of small satellites announced regularly. Many proposed scenarios require high communication bandwidth to be implemented and are often constrained by the limited resources available onboard small spacecraft. In this context, the interest for optical communications for point–to–point links is steadily growing due to the inherent advantages of such technology, that are: (1) much higher bitrate and workable communication distance, compared to traditional RF systems, especially considering inter–satellite links; (2) increased channel security, since laser links are immune to jamming and are virtually impossible to intercept; (3) absence of frequency license regulations, which comes particularly advantageous since RF bands allocation is close to saturation and (4) possibility to implement Quantum Key Distribution protocols to further enhance the communication security.

Stemming from these premises, Stellar Project is developing LaserCube, an optical communication terminal compliant with the CubeSat standard, suitable for integration on nanosatellite platforms starting from the 6 U form factor, though it can be embarked also on larger satellites. LaserCube is designed to transmit and distribute an unprecedented amount of diversified space-borne data. Optical communication will contribute to enable the business opportunities in the growing New Space Economy related to the employment of CubeSats, including Earth imagery, weather forecasting, global telecommunications and internet services, IoT and M2M. Other perspective developments are related to secure communications even through the implementation of quantum communication protocols.

Today, nanosatellites exploit telecommunication subsystems based on UHF, S or X band to transmit data towards ground stations, with bitrates bounded from few kbps to some tens of Mbps [1]. Bitrates up to 220 Mbps have been achieved using proprietary X–band systems in conjunction with several–meter ground antennas [2]. Ka–band is an emerging technology which is not a standard in the nanosatellite community yet [3][4]. As regards intersatellite links between nanosatellites, there have been some recent developments using S–band systems, but the in-flight performance in terms of bitrate are not useful for commercial purposes (1 kbps over few hundred km, [5]).

Thanks to their very narrow beam and short wavelength, laser links are ideal for high bitrate, point–to–point communications. This prompted the development of the few examples of lasercom terminals conceived for nano and micro satellites that can be found in the literature. The most prominent examples are Fibertek [6], CubeCat [7], MIT's NODE [8] and CLICK systems [9], NASA's OCSD [10]. A lasercom system for microsatellite called SOTA has been developed in the last years [11]. Table 1 sum-

*Funding: This work was supported by the European Space Agency ARTES Competitiveness and Growth program – Technology Phase and by the Italian Space Agency [ESA contract 4000121651/17/UK/AD].

*Corresponding author
Email address: francesco.sansone@stellarproject.space (Francesco Sansone)

Nomenclature

ADCS	Attitude Determination and Control Subsystem
AIU	Actuators Interface Unit
APD	Avalanche Photodiode
BCN	Beacon
BER	Bit Error Rate
COTS	Commercial Off The Shelf
DL	Downlink
EM	Engineering Model
FPGA	Field Programmable Gate Array
FSM	Fast Steering Mirror
ISL	Inter-Satellite Link
MCU	Micro Controller Unit
MOS	Miniature Optical Subsystem
MTS	Miniature Telecom Subsystem
PCU	Power Conversion Unit
PEB	Payload Electronic Board
PID	Proportional Integrative Derivative
PSD	Power Spectral Density
QKD	Quantum Key Distribution
SIU	Sensors Interface Unit
SNR	Signal to Noise Ratio
SPIN	Stabilization and Pointing Instrument for Nanosatellites
TLC	Telecom
TRL	Technology Readiness Level

Table 1: Lasercom terminals for nano and micro satellites.

System	Mass [kg]	Volume [U]	Power [W]	Bitrate [Mbps]	TRL
Fibertek	2	2	20	1000 (DL)	8
OCSD	1	0.5	15	200 (DL)	9
CubeCat	1.3	1	15	1000 (DL)	< 7
NODE	1	1.2	15	$10 \div 100$ (DL)	7
CLICK	1	1.2	15	10 (DL) ≤ 18 (ISL)	< 7
SOTA	5.9	n.a.	28	10 (DL)	9
LaserCube	<1.8	2	18 20	1000 (DL) ≤ 100 (ISL)	6

marizes the main facts relative to the systems mentioned above. Data on the LaserCube terminal are expected for the flight model; in the mass breakdown, mass of the terminal optomechanical unit is already establshed, while the mass of the electronic unit is estimated with a good level of confidence (more in Sec. 3). The same applies for the terminal volume.

The mentioned lasercom systems rely on the host satellite ADCS for coarse pointing, and are usually provided with a fine pointing stage for laser beam fine alignment. In fact, one of the most challenging aspects related to free-space optical communication over long distances is the required pointing accuracy that is needed to establish a laser link, due to the extreme narrowness of collimated laser beams (typically between 1 and 100 µrad).

State of the art of small spacecraft attitude control technology is capable to achieve a pointing accuracy below 1.7 mrad, with peak performance as low as 122 µrad [12]. Recently, high pointing accuracy has been demonstrated by small–satellite missions dedicated to astronomical observations. NASA–JPL Arcsecond Space Telescope Enabling Research in Astrophysics (ASTERIA) is a 6U nanosatellite capable of achieving 2.4 µrad rms of static pointing stability, by exploiting an accurate commercial ADCS, and a custom fine–pointing piezo stage [13]. Other examples include the red3 U Miniature X–ray Solar Spectrometer (MinXSS) by University of Colorado Boulder [14], and the BRITE constellation composed of six cubic vehicles [15].

The mentioned missions are dedicated to static observations of far objects, while optical communication systems generally deal with dynamic pointing requirements, especially during ground station tracking in downlink scenarios, or out–of–plane intersatellite links. Slew rates are typically around 20 mrad/s on 400 km orbits [16], greatly stressing the satellite ADCS and making pointing more challenging compared to static observations. In addition, the need of satellite steering for telecommunication purposes may affect or prevent other primary tasks requiring different attitudes, such as imaging.

In this paper, the authors present the results of the development of LaserCube, a lasercom terminal for small satellites that provides unprecedented communication capabilities without requiring cutting–edge ADCS. Section 2 describes the LaserCube architecture and in Sec. 3 the LaserCube Engineering Model is presented. Section 4 explains pointing control system scheme and design process. Section 5 summarizes the main results from the validation test campaign of the LaserCube EM. A feasibility study relative to the implementation of Quantum Key Distribution protocols with LaserCube is presented in Sec. 6. Conclusions are given in Sec. 7.

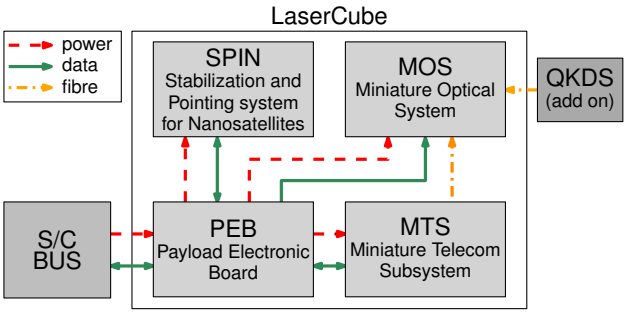

Figure 1: LaserCube top–level architecture and main subsystems.

Table 2: LaserCube–ISL and LaserCube–DL main figures.

Parameters	LC–ISL	LC–DL
Size	2 U	2 U
Mass	<1.8 kg	<1.8 kg
Power	20 W	18 W
Wavelength (TLC)	915 nm	1550 nm
Wavelength (BCN)	808 nm	808 nm
Aperture	40 mm	40 mm
Pointing range	± 10°	± 10°
Pointing accuracy	<10 µrad rms	<10 µrad rms
Beamwidth	30 µrad rms	50 µrad rms

2. LaserCube System Overview

LaserCube is a miniature, two–way optical communication system compliant to the CubeSat standard and conceived for nano-, micro- and mini-satellites. It is intended to provide a step–change in communication capabilities of miniature orbital platforms by the exploitation of optical communications. LaserCube tackles the pointing issue with a dedicated dual–stage pointing system. The latter is based on (1) a coarse mechanism capable to achieve a pointing accuracy of 60 µrad rms or better, and (2) a fine pointing stage that corrects laser steering down to 10 µrad rms. The coarse pointing system (SPIN) is based on an innovative technology patented by Stellar Project [17]. SPIN relieves the host satellite attitude control system from performing precise pointing and achieves coarse pointing accuracy much better than the attitude pointing accuracy of nano- and microsatellites equipped with star trackers (∼0.5 mrad), thus making possible to use COTS hardware for CubeSat ADCS without dedicated star trackers.

2.1. LaserCube Architecture

LaserCube is conceived to support optical communications in both downlink (DL) and intersatellite link (ISL) applications. The LaserCube top–level architecture is modular and based on the building blocks shown in Fig. 1, which are common to both the intersatellite link configuration (LaserCube–ISL) and the downlink configuration (LaserCube–DL). The main figures of the LaserCube variants are summarized in Tab. 2.

The Stabilization and Pointing Instrument for Nanosatellites (SPIN) is responsible for orienting the optical sub–unit (MOS) with high accuracy (in the order of 60 µrad rms) towards the direction connecting two LaserCube units, while rejecting disturbances due to satellite attitude jitter and micro–vibrations. SPIN is the primary stage of the dual stage pointing system of LaserCube. The Miniature Optical Subsystem (MOS) performs a dual task: collect laser light coming from the remote terminal (both telecom and beacon signals) on dedicated optical sensors and generate two laser beams (telecom and beacon). It features a fine–pointing mirror which constitutes the second stage of the dual stage pointing system. The Miniature Telecom Subsystem (MTS) comprises all the elements that are needed to generate an optical carrier, modulate the carrier with On/Off Keying scheme, and detect the received signal. The Payload Electronic Board (PEB) manages power conversion and distribution, exchanges data with the satellite bus and manages the control of the dual stage pointing system actuators. The Quantum Key Distribution Subsystem (QKDS) is dedicated to transmission of quantum–encryption keys in a downlink scenario; it is conceived as an add–on to LaserCube and has been subjected to a feasibility study. LaserCube–ISL features a full duplex (TX and RX) communication channel, to allow mutual data exchange between two satellites. Considering space–ground applications, the use of standard RF systems is considered for data uplink, due to the relatively low data volume of telecommands; instead, data streams from LEO to ground are much higher due to the need of transmitting large amounts of spaceborne data (e.g. high resolution images). Therefore, the development of the LaserCube–DL EM does not include a receiver optical termination. All LaserCube units are provided with a dedicated laser that acts as beacon for the parent unit (either another LaserCube unit or an optical ground station).

2.2. Operational scenarios

Orbital considerations in DL and ISL scenarios determine the pointing mechanism requirements in terms of maximum rotation angle and slewing rate.

In the first case, the system is used to transmit spaceborne data (e.g. high resolution or multispectral images gathered by optical payloads) towards an optical ground station in the visibility time window between the satellite and ground segment. Orbital parameters such as altitude, inclination and eccentricity determine the link availability. Considering (almost) circular, high inclination (e.g. polar) orbits with typical altitudes between 500 km and 700 km, and a minimum elevation angle over the local horizon of 15 deg, typical link availability is in the order of 400 s. During this period, a slewing maneuver is executed in cooperation between the satellite and the LaserCube coarse pointing system: the satellite rotates in order to point towards the ground station during the whole pass with a maximum pointing error of 10 deg, while LaserCube aligns itself towards the ground station compensating the pointing error of the satellite. In this situation, the satellite shall perform a manoeuvre close to 150 deg (±75 deg) with an

average slewing rate between 4 and 8 mrad/s, while LaserCube performs a 20 deg (±10 deg) rotation with a slewing rate between 1 and 2 mrad/s.

In ISL scenarios, the system is used to transmit / receive data over optical channel with satellites placed on the same orbital plane. Ideally, in circular orbits the relative dynamic is null; in practice, non–ideal placement of satellite in their nominal orbital positions as well as other non–linear effects due to the Earth gravity field result in variation of the line of sight connecting two satellites on the same orbit. Such variation can sum up to ±4 deg, with main motion harmonic related to the orbital period (approximately 90 min at 500–700 km of altitude). Typical values of relative angular velocity are on the order of 80 µrad/s.

Differently, the design requirements in terms of pointing accuracy come from the link budget, as a function of laser beam divergence. In ISL mode, LaserCube is designed to guarantee 100 Mbps with a 1000 km baseline or 10 Mbps at 2000 km, with beam divergence of 30 µrad. In order to minimize pointing losses, the pointing requirement becomes ±10 µrad rms. Even though the telecom laser of the LaserCube Downlink version has a slightly larger beamwidth (50 µrad), the same requirement on the pointing accuracy is applied to minimize losses and keep the same configuration of the pointing system.

Regardless of the communication link mode, the pointing performances have to be achieved in a disturbed environment. The main perturbations that affect a laser communication terminal on a satellite come from the bus oscillations (attitude jitter) due to its attitude control limitations and micro–vibrations caused by the operation of moving parts onboard the satellite (e.g. reaction wheels for attitude control or flexible antennas and solar panels). Not many orbital data are available in the literature on the microvibration environment and attitude jitter onboard regular–size satellites, and, to the best of the authors' knowledge, no data can be found for nano- or microsatellites. The microvibrations onboard the Japanese satellite OICETS (570 kg) have been estimated in [18] starting from the micro–accelerations measured on orbit by a dedicated instrument on the satellite. This is of particular interest since OICETS carried an experimental optical communication terminal for downlink experiments [19]. Estimated microvibrations in the 0.1–1000 Hz range vary from 10^2 to 10^{-8} µrad^2/Hz, with PSD (Power Spectral Density) basically falling with frequency to the fourth. Since LaserCube is conceived for satellites bewteen four and fifty times lighter than OICETS, the results presented in [18], although a valuable benchmark, are not considered applicable a priori to this work. Therefore, the microvibration environment onboard nano or microsatellites has been estimated by means of controlled attitude simulations of a 10 kg miniature satellite in LEO [20, 21]. The simulated vehicle is equipped with an attitude determination and control system based on commonly available technology: three reaction wheels for disturbance rejection and three magnetic torque rods for desaturation of the wheels. The numerical model takes into account the effects of the gravity gradient, the interaction between the satellite and the Earth magnetic field, attitude sensors errors and the disturbances induced by flexible solar arrays. Results can be found in [22] and are comparable with the data provided by [18].

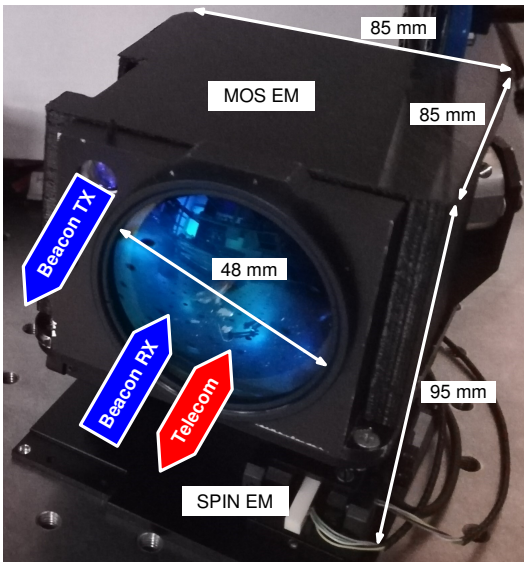

Figure 2: LaserCube Opto–Mechanical Unit, including the SPIN EM and the MOS EM.

3. LaserCube Engineering Model

This section describes the Engineering Model of the LaserCube variant for intersatellite links. The LaserCube EM Opto–Mechanical Unit, including SPIN and MOS, is shown in Fig. 2. The LaserCube Electronic Unit comprises the MTS and PEB breadboards, which are shown in Fig. 4 and Fig. 5, respectively.

The SPIN Engineering Model consists of a two rotational degrees–of–freedom (elevation and azimuth) parallel

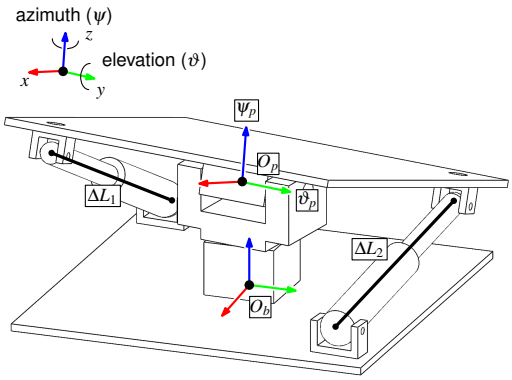

Figure 3: Mechanical scheme of the SPIN Engineering Model. The base–fixed reference frame, O_b, and the platform reference frame, O_p, are shown. The elevation, ϑ, and azimuth, ψ, angles are uniquely determined from the legs elongation values, ΔL_1 and ΔL_2.

platform, which is composed by a moving base that is connected to the host satellite structure by means of a central universal joint and two extensible links (see Fig. 3). The angular position of the moving platform is imposed by controlling the position of two linear actuators embedded in the extensible links; thus, the controlled movement of the platform serves as coarse pointing (accuracy: 60 µrad rms, range: ±10 deg) of the MOS along elevation and azimuth angles, while reducing the disturbances coming from the satellite bus. The SPIN actuators are commercial linear walking piezo–motors with embedded optical sensors (position resolution <1 nm, encoder resolution 1.25 µm). The SPIN mechanism joints are all based on flexural pivots in order to avoid backlash, friction and lubrication. Moreover, they benefit of a large operational temperature range and simplicity. The SPIN technology is patented by Stellar Project [17]. The SPIN EM is fully representative of the flight model in terms of volume, mass and performance. Its envelope is roughly 0.4 U and its mass less than 0.3 kg.

The MOS Engineering Model is composed by the following elements: (1) a 40 mm aperture main lens, (2) a fast–steering mirror (FSM) based on a commercial piezo tip/tilt platform, (3) a dichroic mirror reflective for wavelengths greater than 850 nm, that separates the optical path of the incoming beacon laser at 808 nm and the telecom laser at 915 nm, (4) a commercial silicon quadrant detector that is used to detect the beacon beam and provides information on the optical unit pointing error, (5) a fiber–to–free–space adapter to connect the MOS to the MTS and (6) a fiber collimator lens from which the beacon laser is sent towards the remote terminal (another LaserCube unit or a ground station). Transmitted telecom signals are reflected by the dichroic mirror onto the FSM and then towards the main lens; part of this optical path is shared by received beacon signals, which enter the main lens, are reflected by the FSM and then pass through the dichroic mirror and are focused on the beacon detector. The choice of a lens with respect to a mirror–based design is dictated mainly by considerations on the size and payload occupancy, since with this solution the inner part of the optical unit is let free for other components (e.g. the fast–steering mirror). Moreover, the obstruction of the reflector mirror in the telescope would introduce an additional power loss. The transmitted beacon beam does not pass through the main optical path in order to avoid saturation of both beacon and telecom detectors due to unwanted back-reflection, given that the transmitted beacon laser power is several orders of magnitude grater than received signals. The same issue for the telecom laser is avoided adopting time division between transmission and reception. The fast–steering mirror is also used as point–ahead system for the telecommunication laser. Point–ahead due to the finite speed of light can sum up to 8 µrad in ISL scenarios considering satellites on the same orbital planes in LEO and up to 50 µrad in DL scenarios. Such values are well within the fast steering mirror angular range (±1000 µrad), therefore the fine pointing system can impose an angular offset between the incoming beacon laser and the transmitted telecom laser in order to provide the necessary point ahead. The quadrant detector is used as beacon sensor to provide the pointing control algorithm with a measure of the pointing error. The device has a total field of view of ±15 millirad, which is much larger than the fast–steering mirror field of regard specified above. The MOS EM fits in less than 0.5 U and weights less than 0.4 kg.

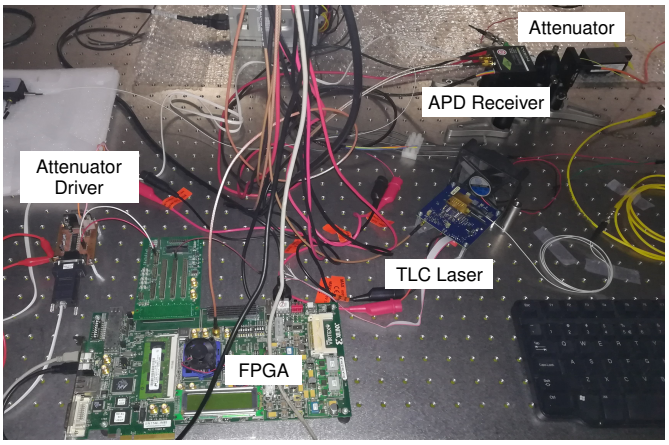

Figure 4: Miniature Telecom Subsystem Breadboard. The variable attenuator and its driver are part only of the test setup and they are used to simulate the signal attenuation corresponding to ISL distances.

The MTS breadboard features all the functional elements of one intersatellite link, which are: (1) a FPGA for data encoding and generation of the modulation signal for the telecom laser carrier, (2) the telecom laser and the beacon laser sources with their drivers and (3) the avalanche photodiode used as telecom receiver, with integrated electronics for signal conditioning. Modulation of the telecom laser carrier is performed through direct modulation of the laser current. This design solution was preferred for LaserCube-ISL since it is simpler and more compact compared to the use of a low–power source coupled with an optical amplifier. The required 2 W laser carrier can be obtained by commercial semiconductor lasers. Carrier modulation through external optical modulator is also discarded since commercial optical modulators accept input power only up to few hundreds mW. Nevertheless, the Downlink version of the terminal will use a continuous wave laser source and an optical amplitude modulator to obtain modulation of the laser carrier at GHz level. The consequent reduction in optical transmit power is tolerated since a relatively large optical aperture (up to 1 m) will be available at the ground station receiver. The MTS breadboard is purely based on commercial hardware and thus it is not fully representative of the flight model in terms of mass and size. In the LaserCube Flight Model, whose design is now advanced, the MTS elements are integrated on two PC104 electronic boards, for a total mass and volume of 0.3 kg and 0.3 U.

The PEB breadboard is composed by the Actuators

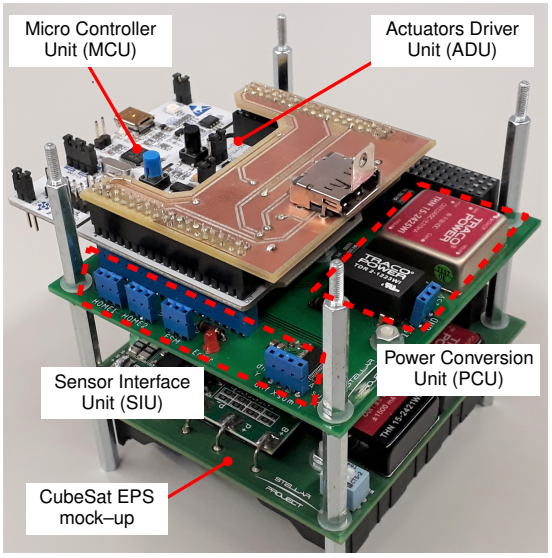

Figure 5: Payload Electronic Board Breadboard. FSM driver is not shown. The lower board is a CubeSat Electric Power System mock-up that is not actually part of the PEB.

Interface Unit (AIU), the Sensor Interface Unit (SIU), the Micro–Controller Unit (MCU) and the Power Conversion Unit (PCU). The MCU is responsible of handling the whole operation of the dual stage pointing system, which includes SPIN and the FSM. The control algorithm uses the signal provided by the laser beacon detector to control the LaserCube pointing direction with respect to the laser beam coming from another terminal. Secondary tasks of the MCU include the handling of data and commands exchanged with the host computer, data–logging for diagnostic purposes, and system status monitoring. The Actuators Interface Unit comprises all the electronics required to drive the SPIN linear actuators and the piezoelectric tip/tilt platform of the fine pointing system that is inside the MOS. The SIU is dedicated to the conditioning and acquisition of the system internal sensors, i.e. the beacon detector, the linear actuators encoders and the FSM stain gauges. The Power Conversion Unit provides the required regulated power supply to all the components of the PEB; it receives three power lines from the satellite bus: 3.3 V, 5 V and 12 V, which are quite common on CubeSat platforms. In the flight model, the PEB elements will be integrated in three PC104 electronic boards, for a total mass of 0.35 kg and volume of 0.4 U. The Electronic Unit, comprising the stack made of the MTS and PEB boards as well as a surrounding aluminum frame, will have an overall mass of 0.9 kg and volume of 1 U ($95 \times 95 \times 95$ mm^3).

Table 3 presents the technical budgets for all the subsystems of the LaserCube–ISL EM, including preliminary data for the QKDS. The expected performance of the EM are presented in Fig. 6 in terms of estimated Bit Error Rate (BER) vs intersatellite link distance for different bitrate values. Table 4 describes the main EM parameters which have been used to estimate the ISL performance.

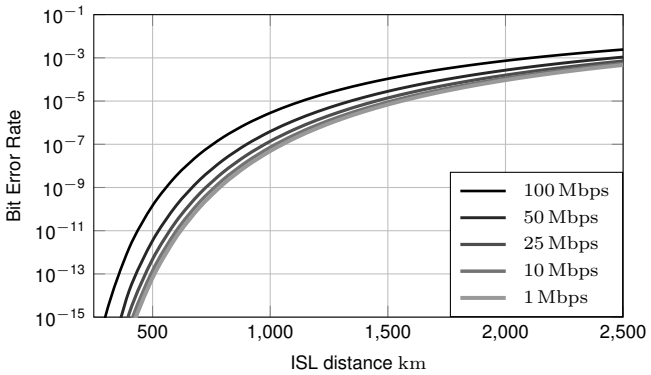

Figure 6: Simulated BER vs ISL distance for different bitrates, taking into account internal optical losses measured in laboratory.

4. Pointing Control System

The architecture of the LaserCube dual-stage laser beam-tracking controller and pointing accuracy test results are described in detail in [22] and summarized here briefly. The primary and secondary stages are controlled by two independent digital controllers, both of the PID type. The former computes the orientation (i.e. elevation and azimuth) reference of the SPIN, which is then converted into an elongation reference for the two linear piezo–motor servo–drives by resorting to the inverse kinematic function of the primary stage. The latter, instead, directly provides

Table 3: LaserCube–ISL EM and QKDS technical budgets.

Subsystem	Mass [kg]	Power [W]	Size [mm^3]
SPIN	0.28	3-5	$91 \times 91 \times 40$
MOS	0.39	6-9	$85 \times 85 \times 55$
MTS	0.55	3-5	∼0.5 U
PEB	0.30	2-3	$95 \times 90 \times 40$
harness and fibers	0.10	n.a.	n.a.
QKDS (preliminary)	0.30	3-5	$95 \times 90 \times 40$

Table 4: LaserCube–ISL EM main figures.

Parameter	Value	Units	Notes
Transmitter			
Telecom optical power	2	W	
Telecom wavelength	915	nm	
Beacon optical power	2	W	
Beacon wavelength	808	nm	
Optical aperture	0.04	m	
Laser beamwidth	30	µrad	
Transmit optical losses	2.15	dB	measured
Pointing accuracy	5	µrad	1σ
Receiver			
Optical aperture	0.04	m	
Receive antenna gain	102.76	dB	
Receive optical loss	2.55	dB	measured
APD responsivity	0.44	A/W	from datasheet
APD gain	150	-	from datasheet
APD dark current	15	nA	from datasheet
APD rise time	1.5	ns	from datasheet
Excess noise factor	4.95	-	
Noise bandwidth	500	MHz	

an orientation reference to the servo–drive of the secondary stage. The two controllers cooperate to focus the incoming laser beam on the optical sensor, so that the pointing error is within specifications. Their design is accomplished by applying the *sensitivity decoupled method* proposed in [23, 24], which allows to independently address the control design of the two stages. The separation of the two designs is achieved by feeding the primary stage controller with the orientation error of the primary stage, obtained by subtracting from the total orientation error provided by the optical sensor the actual orientation of the secondary stage, which is measured with ad hoc strain–gauges integrated within the secondary piezo–stage. The PID controllers are designed with conventional frequency response methods, in order to meet the desired tracking accuracy while facing the typical noise sources affecting the performances of the control system. These are identified as the encoders quantization noise of the two linear motors, the output noise of the optical sensor, and the jitter motion of the satellite bus. Both the encoders quantization and the optical sensor measurement errors can be considered as white noises, while the satellite bus jitter is modeled as a noise with the spectrum envelope estimated as described in [20][21] (see also Sec. 2.2). An error budget analysis is performed both to determine how much each noise source contributes to the overall tracking error, and to shape the sensitivity functions of the two control loops (primary and secondary) to get the noise attenuation required by the design specifications. The design is carried out in continuous–time, and then discretized with conventional methods, eventually yielding a dual-rate control configuration. The implementation of the PID controllers includes an integrator anti–windup scheme, to prevent unnecessary accumulation of tracking error during large positioning transients.

5. System Validation

A laboratory validation campaign has been carried out with the goal of demonstrating the critical functions and performance of the LaserCube Engineering Model, in particular (1) the pointing, tracking and satellite attitude jitter rejection capability of the dual stage pointing system and (2) the intersatellite link performance in terms of bitrate and bit error rate.

The test bed shown in Fig. 7 has been set. It features (1) the LaserCube Opto-Mechanical Unit (SPIN and MOS EMs) mounted on top of a pan/tilt unit that is used to impose to the SPIN base a motion that is representative of the attitude jitter of small satellites as discussed in Sec. 2.2 and in Sec. 4, (2) the PEB controlling the OMU, (3) one simplified MOS breadboard providing the laser beacon that simulates the presence of a remote LaserCube unit, (4) the MTS breadboard, comprising the transmission section (FPGA or signal generator, 915 nm pigtailed laser telecom and its driver, optical variable attenuator and its driver) connected to the MOS EM and the receiver section (APD receiver, oscilloscope) connected to the MOS breadboard, as shown in the box in the center of Fig. 7 and in Fig. 9 and finally (5) the ground segment equipment (power supplies and one PC to monitor the experiment). The whole experiment is mounted on an optical table with vibration isolation.

5.1. Pointing Accuracy

Verification of the pointing and tracking accuracy of the LaserCube dual stage pointing system under dynamic conditions that are representative of the operational scenario onboard small satellites was carried out using the elements highlighted in red in Fig. 7. A detailed description of the test procedure and results is provided in [22]; in this paper the main results are graphically summarized in Fig. 8. The selected disturbances always have an amplitude larger or equal to the estimated satellite attitude jitter envelope (solid gray line). According to the test results, the pointing accuracy is always between 3 and 10 µrad std in the whole frequency range ($0.01 \div 10$ Hz) of the imposed excitation. The corresponding disturbance attenuation ranges from -45 dB to -5 dB.

5.2. ISL Telecom Performance

The functional scheme of the telecommunication setup is presented in Fig. 9. The laser driver modulates the optical power of the 915 nm telecom laser output by a square wave with variable frequency (1 MHz, 10 MHz, 25 MHz and 50 MHz), which correspond to simulated equivalent bitrates. The square wave of the driver is provided by a FPGA or a signal generator.

The attenuation of the modulated optical signal is set by the variable attenuator controlled by the FPGA in order to simulate different intersatellite link distances. The modulated and attenuated telecom optical signal is fed to the MOS EM and free-space propagated. At the receiving end (MOS BB) it is coupled to either a single mode fiber (core: 6 µm) or a multi–mode fiber (core: 100 µm) and sent to the input of the APD receiver. The differential voltage at the output of the APD receiver is acquired by the oscilloscope where the eye-diagram is shown and BER is estimated. For each modulation rate the eye diagram is shown for several values of received power, from 0.8 µW to 80 nW, which correspond to a range of simulated ISL distance between 370 and 2400 km. The following test procedure was applied.

Eye-diagram measurements have been performed with active and non-active pan/tilt unit.

Preliminarily, to assess the coupling efficiency of the fiber injection from the steering mirror, some tests have been performed with a single–mode fiber, which could be employed for a better compatibility with telecom devices. However, the coupling loss to a single–mode fiber is too high and the eye–diagram measurements showed significant variations of the signal waveform when the pant/tilt unit was active. This is because the focused telecom laser

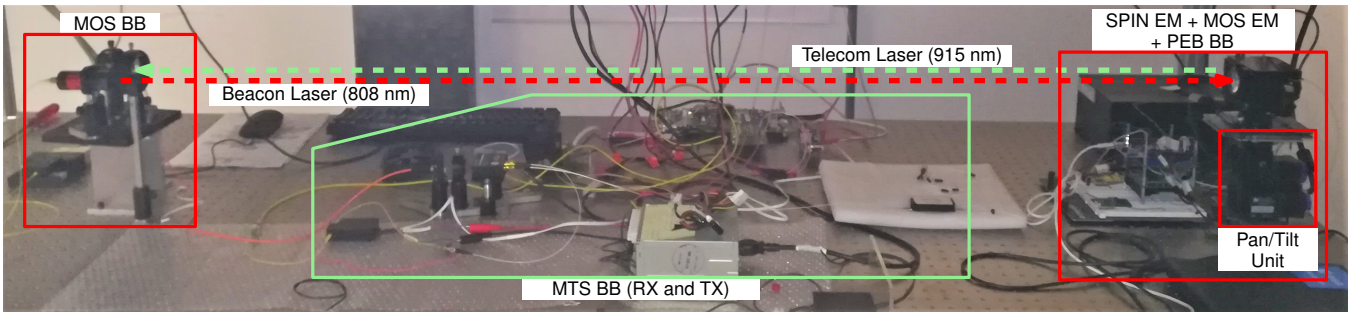

Figure 7: Complete test setup for LaserCube validation tests. Red elements only: testbed for pointing accuracy validation described in [22]. Red and green elements: testbed for telecom performance validation.

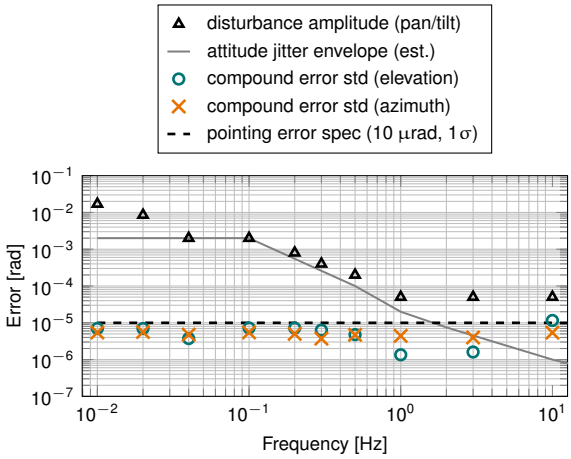

Figure 8: Disturbance rejection tests: compound errors with disturbance on elevation (circles) and azimuth (crosses).

spot at the fiber injection was subjected to lateral displacement in the order on 1–2 µm, which is comparable to the fiber core of 6 µm, resulting in too high pointing losses.

On the other hand, the tests performed with a multi–mode fiber coupling the optical unit to the APD receiver showed that no appreciable signal degradation were measured with the pant/tilt unit activated. This is because, in this case, the pointing loss were negligible since pointing accuracy was much smaller than the fiber core diameter. Also, slight improvement of BER can be appreciated since the multi–mode fiber can collect more energy and thus provide a higher signal–to–noise ratio. Multi–mode fiber is selected for the final design.

BER estimation with the use of the multi-mode fiber at the receiver section for different simulated ISL distances is summarized in Fig. 10a to Fig. 10d. Unfortunately, tests with telecom laser carrier modulation of 25 MHz were carried out only using the FPGA to generate the modulation signal; the other modulation rated were imposed using both the FPGA and the laboratory signal generator.

A good correspondence between expected results (dashed plots) and experimental results obtained with the signal generator can be appreciated.

A discrepancy can be appreciated between the expected theoretical BER and the experimental results, when the laser driver is controlled by the signal generated by the FPGA, especially at the lower bitrates (1 Mbps and 10 Mbps). This was due to an unwanted amplitude modulation with low-frequency components of the driving signal, superimposed to the useful OOK modulation. The nature of this electrical signal disturbance was not clearly identified. The experimental results obtained with the FPGA for 25 Mbps and 50 Mbps show a good match with theoretical values.

6. Quantum Key Distribution Feasibility Study

In this section, the assessment of the feasibility of the inclusion of a Quantum Key Distribution subsystem to LaserCube is briefly presented. The QKDs is dedicated to transmission of quantum–encryption keys to enhance communication security. The state of the art suggests that the best choice to implement a QKD system in free space is based on the use of the polarization of single photons [25][26][27]. Concerning the choice of the specific protocol, the BB84 protocol in the decoy–state version [28] represents the optimal choice between security and reliability of the implementation. Indeed, the decoy BB84 protocol requires strongly attenuated (to the single photon level) laser pulses and not "true" single photon states as proposed in the original version of the BB84 protocol [29], whose realization would require more resources in terms of costs and difficulty of the implementation. The critical parameter for QKD is the Quantum Bit Error Rate (QBER) that is determined by the Signal–to–Noise ratio (SNR), given by the ratio between the number of total detections and the dark plus background counts at the receiver. In order to assess the feasibility of QKD with LaserCube, the relative QKD rate (defined as the rate between secure bits and sent qubits) has been calculated for both downlink and intersatellite link scenarios (see Fig. 11 and Fig. 12, respectively) through application of the link budget. This is a pure number; the absolute key rate (measured in bps) is obtained by multiplying the relative key rate by the qubit repetition rate at the source. In order to realize quantum key distribution, the QKD rate must be positive (if negative, the exchanged key is not secure and must be discarded). Wavelengths of 800 nm and 1550 nm have been considered.

In downlink scenarios, the simulations show that, during daylight, positive key rates can be extracted at 800 nm

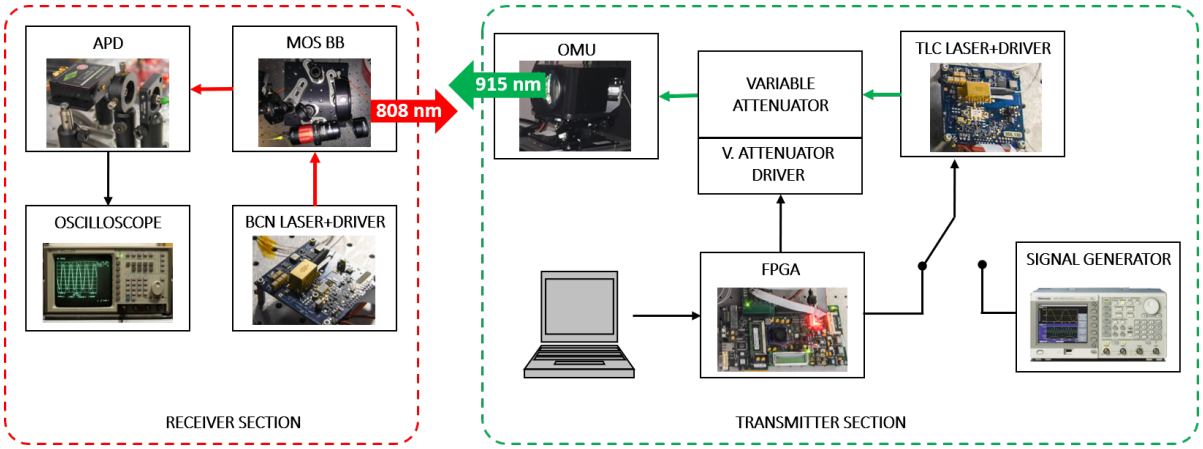

Figure 9: Block diagram of the test setup for verification of ISL telecom performance.

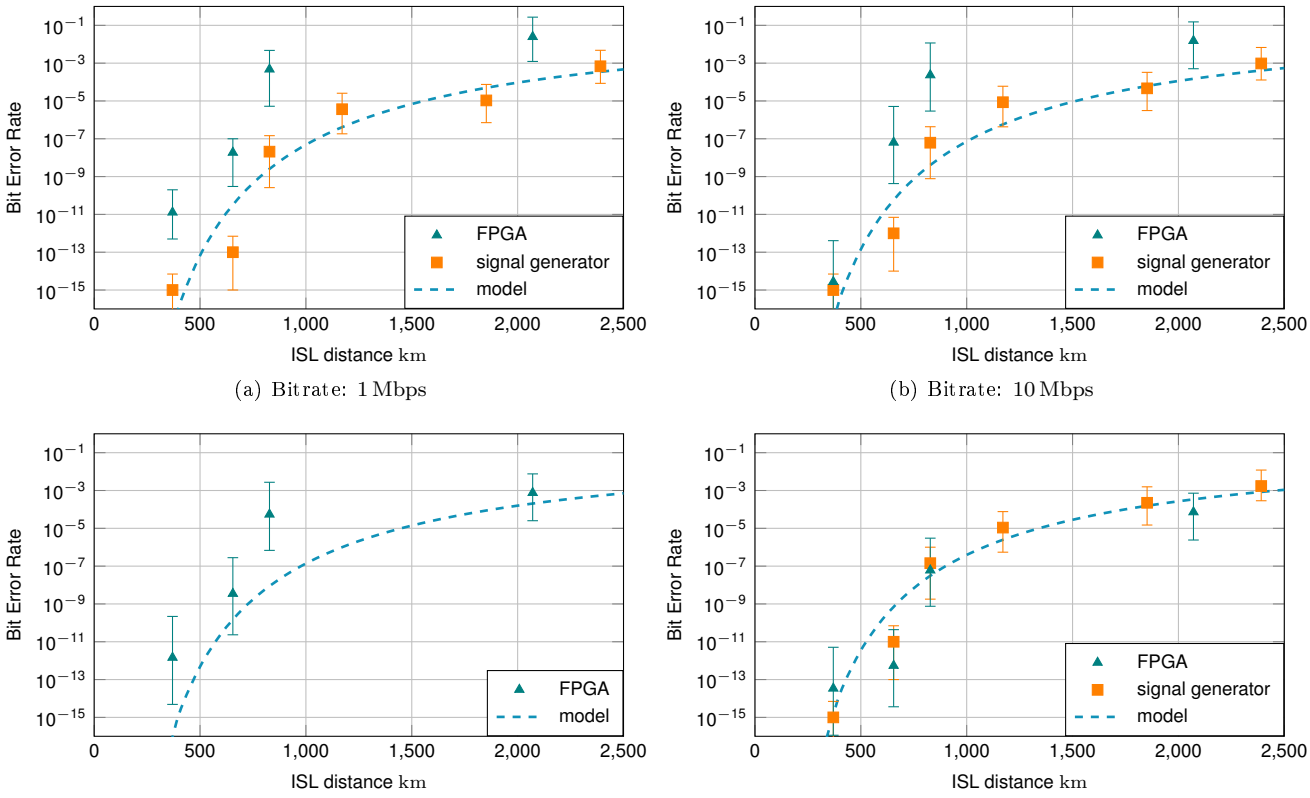

(a) Bitrate: 1 Mbps

(b) Bitrate: 10 Mbps

(c) Bitrate: 25 Mbps

(d) Bitrate: 50 Mbps

Figure 10: BER vs ISL distance: each plot refers to a different value of bitrate. Triangles: modulation with FPGA; squares: modulation with signal generator; dashed line: model from Fig. 6.

only at very short distance (below 600 km), while positive key rates are obtained at 1550 nm for larger distances. Therefore, for daylight operation, the best wavelength is 1550 nm. Considering intersatellite links with diffraction limited beams, positive rates can be achieved. A diffraction limited beam sent by a transmitter with diameter equal to 40 mm results in beam divergence of ∼20 µrad and ∼39 µrad for 800 nm and 1550 nm. These figures (especially 20 µrad) are close to the expected LaserCube pointing accuracy and may result very demanding.

The CubeSat form factor imposes stringent constraints on the QKD applicability. The size of the receiver aperture limits the distance of the ISL for QKD. At 800 nm and by using a diffraction limited beam with a 40 mm diameter aperture at transmitter, the maximal distance is limited to 1000 km; in order to obtain a positive key rate over a 2000 km link, the receiver aperture must be in the order of 150 mm and the transmit beam should be narrower than 50 µrad. Moreover, another issue for the ISL is the difficulty of embarking a QKD receiver into a nanosatellite

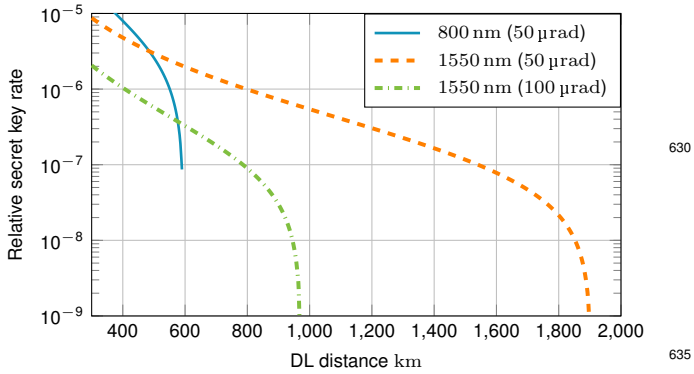

Figure 11: Predicted quantum key rate in a DL scenario for different wavelengths and beam divergence at the transmitter, during sunlight, with a receiver aperture of 400 mm at the ground station.

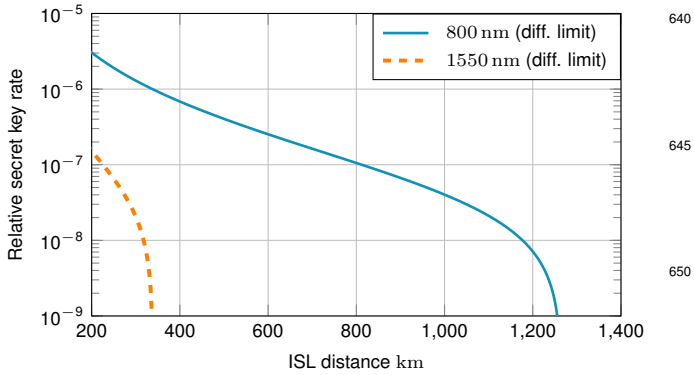

Figure 12: predicted quantum key rate in an ISL link scenario for wavelengths of 800 nm and 1550 nm and diffraction–limited beam divergence (∼20 µrad and ∼39 µrad respectively) at the transmitter, with a receiver aperture of 40 mm onboard.

platform, both in terms of volume and power consumption. Such constraints imply that today QKD applicability on nanosatellite platforms is limited to ISL at low distance and to DL towards ground receivers. On platforms of size ≥6 U QKD over ISL at distances larger than 1000 km may be achieved, if detectors are sufficiently miniaturized and onboard power budget can sustain the receiver section.

7. Conclusions

This paper summarizes the development of the Engineering Model of LaserCube, a laser communication terminal conceived for nano and micro satellites. The EM was subjected to a validation campaign whose goals were (1) the demonstration of unprecedented pointing and tracking capability for a laser communication terminal for small satellites and (2) the demonstration of the expected telecom performance in a simulated intersatellite link scenario. The lasercom EM demonstrated a pointing and tracking capability better than 10 µrad rms in the expected vibration environment. Under such test conditions, the EM was capable of delivering 50 Mbps and 10 Mbps over a simulated intersatellite link distance of 1300 km and 2000 km with BER of 10^{-5} and 10^{-4}, respectively. The link budget model validated through the test campaign shows that 100 Mbps over 1000 km ISL with BER of 10^{-5} can be achieved. The activity also included a feasibility assessment for the integration on the terminal of an add–on package for Quantum Key Distribution, in order to provide enhanced communication security. The next step towards the commercial exploitation of LaserCube is the design and development of the flight model for in-orbit demonstration, which is expected in 2020.

References

[1] B. Klofas, K. Leveque, A survey of cubesat communication systems: 2009-2012, in: 10th Annual CubeSat Developers Workshop, 2013.

[2] K. Devaraj, R. Kingsbury, M. Ligon, J. Breu, V. Vittaldev, B. Klofas, P. Yeon, K. Colton, Dove high speed downlink system.

[3] J. A. King, K. Leveque, M. Bertino, J. Kim, H. Aghahassan, Ka-band for cubesats.

[4] A. Cuttin, F. Alimenti, F. Coromina, E. De Fazio, F. Dogo, M. Fragiacomo, P. Gervasoni, G. Gotti, A. Gregorio, P. Mezzanotte, et al., A ka-band transceiver for cubesat satellites: Feasibility study and prototype development, in: 2018 48th European Microwave Conference (EuMC), IEEE, 2018, pp. 930–933.

[5] L. Léon, P. Koch, R. Walker, Gomx-4-the twin european mission for iod purposes.

[6] M. Storm, S. Gupta, H. Cao, S. Litvinovitch, K. Puffenberger, M. M. Albert, J. Young, D. Pachowicz, T. Deely, Cubesat laser communications transceiver for multi-Gbps downlink, in: 31st Annual AIAA/USU Conference on Small Satellites, 2017.
URL https://digitalcommons.usu.edu/cgi/viewcontent.cgi?article=3684&context=smallsat

[7] R. Saathof, W. Crowcombe, S. Kuiper, N. van der Valk, F. Pettazzi, D. de Lange, P. Kerkhof, M. van Riel, H. de Man, N. Truyens, I. Ferrario, Optical satellite communication space terminal technology at TNO, in: Proc. International Conference on Space Optics, 2018.

[8] C. Payne, A. Aguilar, D. Barnes, R. Diez, J. Kusters, P. Grenfell, R. Aniceto, C. Sackier, G. Allan, K. Cahoy, Integration and testing of the nanosatellite optical downlink experiment, in: 32nd Annual AIAA/USU Conference on Small Satellites, 2018.

[9] P. Serra, O. Cierny, R. Diez, P. Grenfell, G. Gunnison, W. Kammerer, J. Kusters, C. Payne, J. Murphy, T. Sevigny, P. do Vale Pereira, L. Yenchesky, K. Cahoy, M. Clark, T. Ritz, D. Coogan, J. Conklin, D. Mayer, J. Hanson, J. Stupl, Optical communications crosslink payload prototype development for the Cubesat Laser Infrared CrosslinK (CLICK) mission, in: 33rd Annual AIAA/USU Conference on Small Satellites, 2019.

[10] T. S. Rose, D. W. Rowen, S. LaLumondiere, N. I. Werner, R. Linares, A. Faler, J. Wicker, C. M. Coffman, G. A. Maul, D. H. Chien, A. Utter, R. P. Welle, S. W. Janson, Optical communications downlink from a 1.5U Cubesat: OCSD program, in: Z. Sodnik, N. Karafolas, B. Cugny (Eds.), International Conference on Space Optics — ICSO 2018, Vol. 11180, International Society for Optics and Photonics, SPIE, 2019, pp. 201 – 212. doi:10.1117/12.2535938.
URL https://doi.org/10.1117/12.2535938

[11] A. Carrasco-Casado, H. Takenaka, D. Kolev, Y. Munemasa, H. Kunimori, K. Suzuki, T. Fuse, T. Kubo-Oka, M. Akioka, Y. Koyama, M. Toyoshima, LEO-to-ground optical communications using SOTA (Small Optical TrAnsponder) – Payload verification results and experiments on space quantum communications, Acta Astronautica 139 (2017) 377–384. doi:10.1016/j.actaastro.2017.07.030.

[12] NASA, State of the Art of Small Spacecraft Technology - Guidance, Navigation and Control (Dec. 2018).

URL https://sst-soa.arc.nasa.gov/05-guidance-navigation-and-control

[13] M. W. Smith, A. Donner, M. Knapp, C. M. Pong, C. Smith, J. Luu, P. D. Pasquale, R. L. B. Jr., B. Campuzano, J. Loveland, C. Colley, A. Babuscia, M. White, J. Krajewski, S. Seager, On-orbit results and lessons learned from the ASTERIA space telescope mission, in: 32nd Annual AIAA/USU Conference on Small Satellites, 2018.
URL https://digitalcommons.usu.edu/cgi/viewcontent.cgi?article=4067&context=smallsat

[14] J. P. Mason, M. Baumgart, B. Rogler, C. Downs, M. Williams, T. N. Woods, S. Palo, P. C. Chamberlin, S. Solomon, A. Jones, X. Li, R. Kohnert, A. Caspi, MinXSS-1 CubeSat on-orbit pointing and power performance: The first flight of the Blue Canyon Technologies XACT 3-axis attitude determination and control system, Journal of Small Satellites 6 (3) (2017) 651–662.

[15] W. W. Weiss, S. M. Rucinski, A. F. J. Moffat, A. Schwarzenberg-Czerny, O. F. Koudelka, C. C. Grant, R. E. Zee, R. Kuschnig, S. Mochnacki, J. M. Matthews, P. Orleanski, A. Pamyatnykh, A. Pigulski, J. Alves, M. Guedel, G. Handler, G. A. Wade, K. Zwintz, The CCD and Photometry Tiger Teams, BRITE-constellation: Nanosatellites for precision photometry of bright stars, Publications of the Astronomical Society of the Pacific 126 (940) (2014) 573–585. doi:10.1086/677236.

[16] O. Čierny, K. L. Cahoy, On-orbit beam pointing calibration for nanosatellite laser communications, Optical Engineering 58 (04) (2018) 1. doi:10.1117/1.oe.58.4.041605.

[17] F. Sansone, A. Francesconi, Compact stabilized pointing system (WO patent pubblication 2017/115204).

[18] M. Toyoshima, In-orbit measurements of spacecraft microvibrations for satellite laser communication links, Optical Engineering 49 (8) (2010) 083604. doi:10.1117/1.3482165.

[19] T. Jono, Y. Takayama, K. Shiratama, I. Mase, B. Demelenne, Z. Sodnik, A. Bird, M. Toyoshima, H. Kunimori, D. Giggenbach, N. Perlot, M. Knapek, K. Arai, Overview of the inter-orbit and the orbit-to-ground laser communication demonstration by OICETS, in: Proc. of SPIE, Vol. 6457, 2007. doi:10.1117/12.708864.
URL https://doi.org/10.1117/12.708864

[20] F. Sansone, F. Branz, A. Francesconi, A miniature stabilized platform for lasercom terminals on-board nanosatellites, in: 64th International Astronautical Congress, Vol. 10, 2013.

[21] F. Sansone, Technologies for a miniature LEO satellites telecommunication network, Ph.D. thesis, University of Padova, Italy (2015).

[22] R. Antonello, F. Branz, F. Sansone, A. Cenedese, A. Francesconi, High precision dual–stage pointing mechanism for miniature satellite laser communication terminals, IEEE Transactions on Industrial Electronicsdoi:10.1109/TIE.2020.2972452.

[23] M. Kobayashi, R. Horowitz, Track seek control for hard disk dual-stage servo systems, IEEE Transactions on Magnetics 37 (2) (2001) 949–954. doi:10.1109/20.917648.

[24] R. Horowitz, Y. Li, K. Oldham, S. Kon, X. Huang, Dual-stage servo systems and vibration compensation in computer hard disk drives, Control Engineering Practice 15 (3) (2007) 291 – 305, selected Papers Presented at the Third IFAC Symposium on Mechatronic Systems (2004). doi:https://doi.org/10.1016/j.conengprac.2006.09.003.

[25] G. Vallone, D. Bacco, D. Dequal, S. Gaiarin, V. Luceri, G. Bianco, P. Villoresi, Experimental satellite quantum communications, Physical Review Letters 115 (4) (2015) 040502.

[26] S.-K. Liao, W.-Q. Cai, W.-Y. Liu, L. Zhang, Y. Li, J.-G. Ren, J. Yin, Q. Shen, Y. Cao, Z.-P. Li, et al., Satellite-to-ground quantum key distribution, Nature 549 (7670) (2017) 43.

[27] H. Takenaka, A. Carrasco-Casado, M. Fujiwara, M. Kitamura, M. Sasaki, M. Toyoshima, Satellite-to-ground quantum-limited communication using a 50-kg-class microsatellite, Nature photonics 11 (8) (2017) 502.

[28] H.-K. Lo, X. Ma, K. Chen, Decoy state quantum key distribution, Physical review letters 94 (23) (2005) 230504.

[29] C. H. Bennett, G. Brassard, Quantum cryptography: public key distribution and coin tossing., Theor. Comput. Sci. 560 (12) (2014) 7–11.

Biographies

Francesco Sansone is system engineer at Stellar Project. He has a Ph.D. in Space Science and Technology from the Centre of Studies and Activities for Space (CISAS) "G. Colombo" of the University of Padova. His research and professional activities are in the field of systems and technologies for enhancing the capabilities of nanosatellites. This includes laser communication and relative navigation systems. He participated to and supported several research and student projects testing critical technologies in low-gravity environment. Francesco is co-inventor of the LaserCube stabilisation and pointing subsystem and lead engineer for the development of the LaserCube terminal.

Alessandro Francesconi is associate professor of Space Systems at University of Padova. His main research topics are related to spacecraft systems and miniature satellites (with focus on on-orbit servicing, docking and capture of non-cooperative spacecraft, and laser communication), and space debris (where he has 20+ years of experience in studying hypervelocity impacts, satellites collisions and fragmentation). He has been chairman of the Protection Working Group of the Inter Agency Debris Coordination Committee, and he is member of the IAA Permanent Committee on Space Debris. He is co-founder of Stellar Project and co-inventor of the LaserCube stabilisation and pointing subsystem.

Roberto Corvaja graduated in Electronic Engineering at the University of Padova (Italy) in 1990 and received the PhD in Electronic Engineering and Telecommunications at the University of Padova in 1994. Since 1994 he is with the Department of Information Engineering of the University of Padova as assistant professor in telecommunications. His research activity covered several aspects of digital communications, from coherent optical communications systems. to wireless communications and MIMO-OFDM wireless systems. In the last

years his research included massive MIMO systems, quantum communications and free space optical communications.

Giuseppe Vallone is Associate Professor at the University of Padova from 2019. He got his Ph.D. degree in Physics at the University of Torino in 2006. From 2006 to 2011 he worked in the Quantum Optics Group of the Sapienza University of Rome. From 2011 to 2019 he was Assistant Professor at the University of Padova. His research is focused on quantum information, quantum communication, quantum random number generators, Orbital Angular Momentum states. He has more than 100 publications in international journals in the area of quantum optics and quantum information (Researcher ID: H-7579-2012).

Riccardo Antonello received the Laurea Degree (cum laude) in Computer Engineering in 2002 and the Ph.D. in Automatic Control in 2006 from the University of Padova, Italy. He has been a Research Associate at the Dept. of Mechanical and Structural Engineering, University of Trento, Italy, from 2006 to 2010, and then at the Dept. of Management and Engineering, University of Padova, Italy, from 2010 to 2015. Since 2015, he joined the Dept. of Information Engineering, University of Padova, Italy, as a Laboratory Assistant. His research interests lie in the areas of control systems, real-time embedded systems, electric drives and mechatronics.

Francesco Branz is a researcher at the Dept. of Information Engineering and a lecturer in Attitude Control of Satellites at Dept. of Industrial Engineering, University of Padova, Italy. He received his Ph.D. in 2016 at the Center of Studies and Activities for Space "G. Colombo" with a thesis on modeling and control of dielectric elastomer actuators for space robotics. His research also focuses on CubeSat technologies for attitude simulation and control, close range relative navigation and docking systems. He is participating to the development of LaserCube as an external contractor at Stellar Project.

Paolo Villoresi is Full Professor of Experimental Physics at the University of Padova. In 2002 he proposed and realized the first single-photon exchange with a satellite. He founded the QuantumFuture research group, that demonstrated the first Quantum Communication in space using orbiting retroreflectors, polarization and temporal modes, as well as novel QKD protocols and fundamental tests of Quantum Mechanics. He is the Italian delegate in the EU COST action MP1403 Nanoscale Quantum Optics and the deputy delegate for the EU COST action CA15220 Quantum Technologies in Space. He is in the Board of Stakeholders of the European technology platform Photonics21.